Supplementary Material

Arctic stratosphere changes in the 21st century in the Earth system model SOCOLv4

Pavel Vargin*, Sergey Kostrykin, Andrey Koval, Eugene Rozanov, Tatiana Egorova, Sergey Smyshlyaev, Natalia Tsvetkova

*** Correspondence:** Pavel Vargin p_vargin@mail.ru

1 Supplementary

S1. Three-dimensional Plumb flux vectors were calculated according to [Plumb 1985]:

$$F = \left(F_x, F_y, F_z\right) = \frac{p}{p_s} cosy \cdot \begin{pmatrix} V^{*2} - \dfrac{1}{2\Omega a \cdot sin2y}\dfrac{\partial(V^* \Phi^*)}{\partial x} \\ -U^*V^* + \dfrac{1}{2\Omega a \cdot sin2y}\dfrac{\partial(U^* \Phi^*)}{\partial x} \\ \dfrac{2\Omega \cdot siny}{S}\left[V^*T^* - \dfrac{1}{2\Omega a \cdot sin2y}\dfrac{\partial}{\partial x}(T^*\Phi^*)\right] \end{pmatrix}$$

where F_x, F_y, F_z are the longitudinal, latitudinal and vertical components of the Plumb flux vector, with x – longitude, y – latitude, z – altitude, U, V are zonal and meridional velocity, Φ is geopotential, T – temperature, p – pressure, and p_s – pressure at Earth surface, a stands for Earth's radius, Ω for Earth's angular velocity, with $S = \frac{\partial \bar{T}}{\partial z} + \frac{\kappa \bar{T}}{H}$ is static stability, $\kappa = {}^{R}/_{c_p} \approx$0.286 and H represents scale height; a star indicates the deviation from the zonal average and a bar the zonal mean.

Zonal average of three-dimensional Plumb flux is equal to the EP flux.

S2. Residual meridional circulation (RMC) in this study is understood within the feamework of the transformed Eulerian mean approach, first introduced by Andrews and McIntyre (1976). This approach provides diagnostics of wave impacts on the mean flow, and gives the ability to calculate the meridional transport of mass and tracers in the atmosphere. The meridional and vertical components of the RMC are calculated using standard formulas (e.g., Koval et al., 2021):

$$\bar{v}^* = \bar{v} - \frac{1}{\partial\bar{\theta}/\partial z}\left(-\frac{\overline{v'\theta'}}{H} + \frac{\partial \overline{v'\theta'}}{\partial z} - \frac{\overline{v'\theta'}}{\partial\bar{\theta}/\partial z}\frac{\partial^2\bar{\theta}}{\partial z^2}\right),$$

$$\bar{w}^* = \bar{w} + \frac{1}{a\cos\varphi}\frac{1}{\partial\bar{\theta}/\partial z}\left(-\sin\varphi\,\overline{v'\theta'} + \cos\varphi\left(\frac{\partial\overline{v'\theta'}}{\partial\varphi} - \frac{\overline{v'\theta'}}{\partial\bar{\theta}/\partial z}\frac{\partial^2\bar{\theta}}{\partial z\partial\varphi}\right)\right),$$

where a — is the radius of the Earth; $H = RT/\mu g$ is the pressure scale height; R is the universal gas constant, T is the temperature, μ is the molar mass of the atmosphere, g is the acceleration due to gravity. In accordance with formulas (1) and (2), the RMC components consist of two terms: the advective (Eulerian mean) circulation and the wave-induced eddy addition.

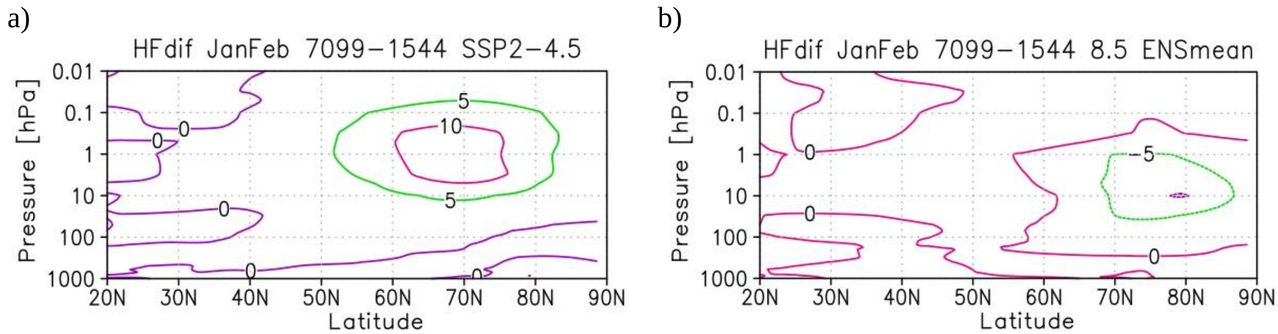

Supplementary Figure S3. Zonal mean heat flux (K m/s) differences of ensemble means in January-February between time periods of 2070-2099 and 2015-2044 under SSP2-4.5 (a) and SSP5-8.5 (b) scenarios.

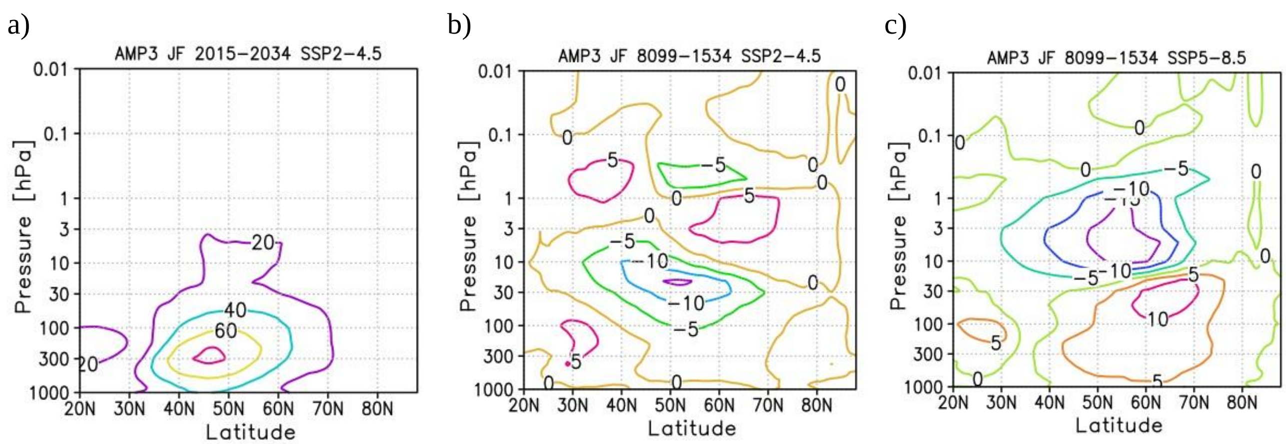

Supplementary Figure S4. Amplitude of wavenumber 3 (gpm) averaged over January-February 2015-2034 under SSP2.4-5 (a). The difference in amplitude of wavenumber 3 (gpm) in January-February between the 2080-2099 and 2015-2034 time periods under the SSP2.4-5 (b) and SSP5.8-5 (c).

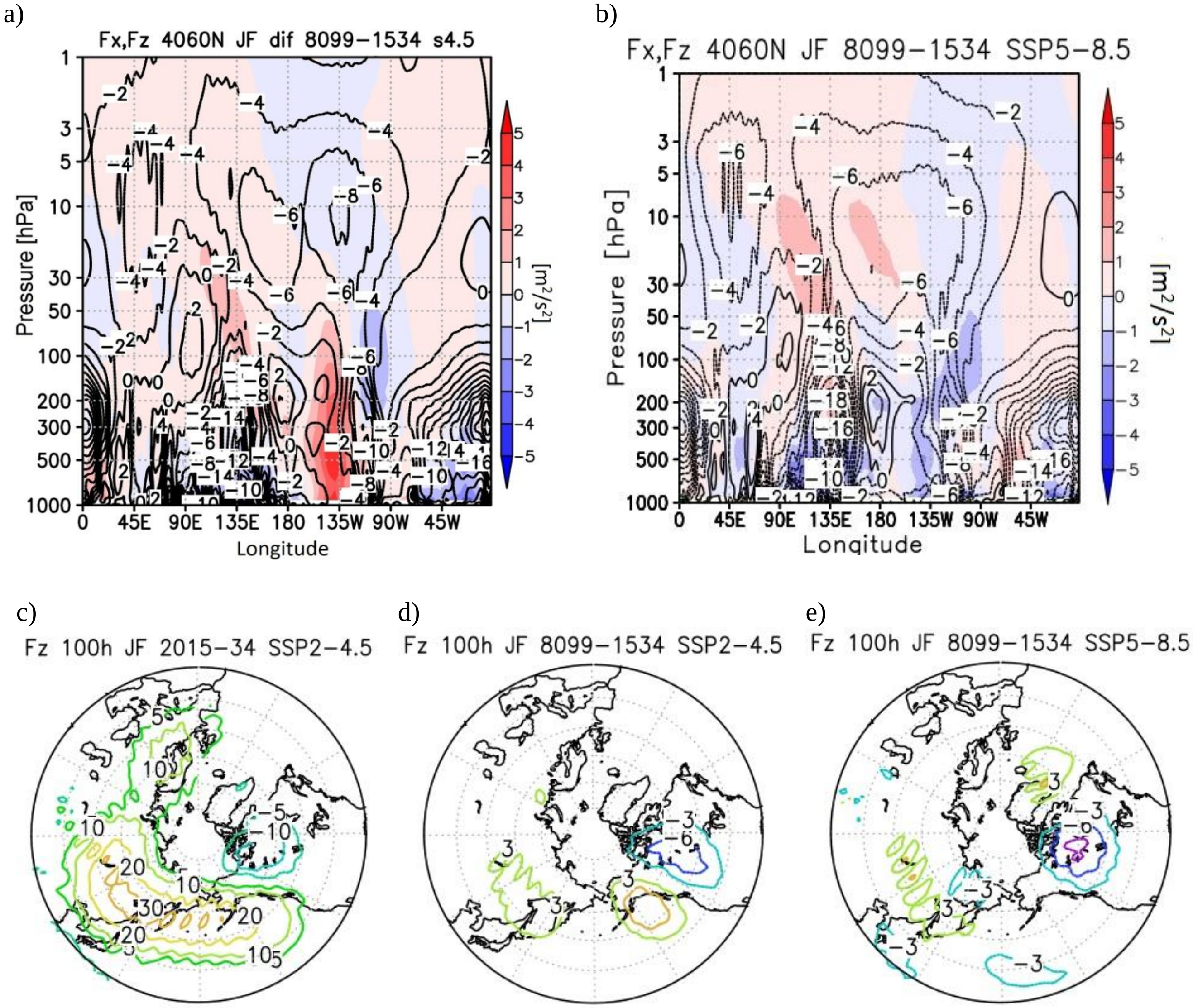

Supplementary Figure S5. Altitude-longitude cross-section of F_x (m^2/s^2) (colors) and F_z component (m^2/s^2 10^{-2}) (black lines) of Plumb fluxes increment in January-February averaged over 40°N-60°N under SSP2-4.5 (a) and SSP5-8.5 scenario (b). Plumb vertical component Fz ($m^2/s^2 \cdot 10^{-2}$) at pressure levels 100 hPa in January-February 2015-2034 under SSP2.4-5 (c), Fz difference between the 2080-2099 and 2015-2034 time periods under SSP2-4.5 and SSP5.8-5 (d, e).

a)

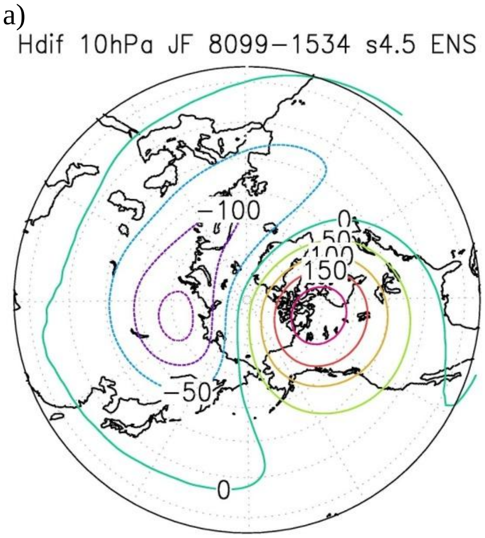
Hdif 10hPa JF 8099−1534 s4.5 ENS
−100
0
150
−50
0

b)

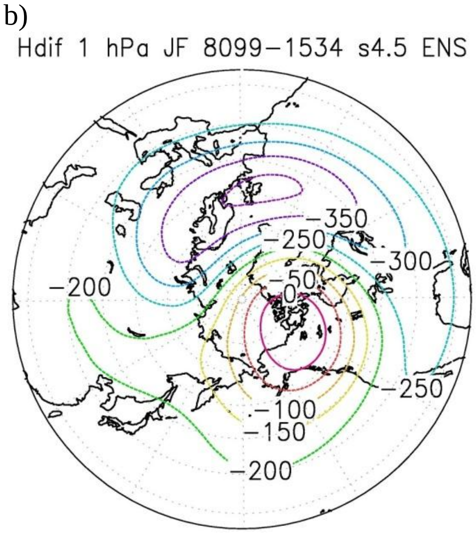
Hdif 1 hPa JF 8099−1534 s4.5 ENS
−350
−250
−300
−200
−50
0
−250
−100
−150
−200

c)

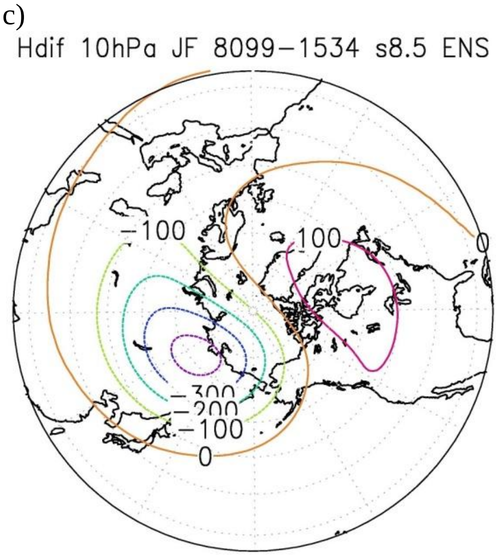
Hdif 10hPa JF 8099−1534 s8.5 ENS
−100
100
0
−300
−200
−100
0

d)

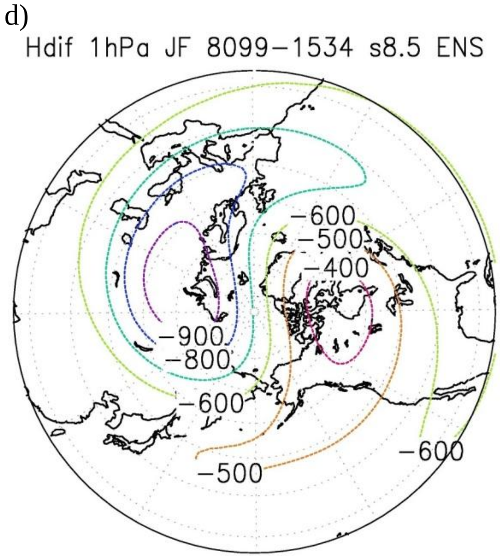
Hdif 1hPa JF 8099−1534 s8.5 ENS
−600
−500
−400
−900
−800
−600
−600
−500

e)

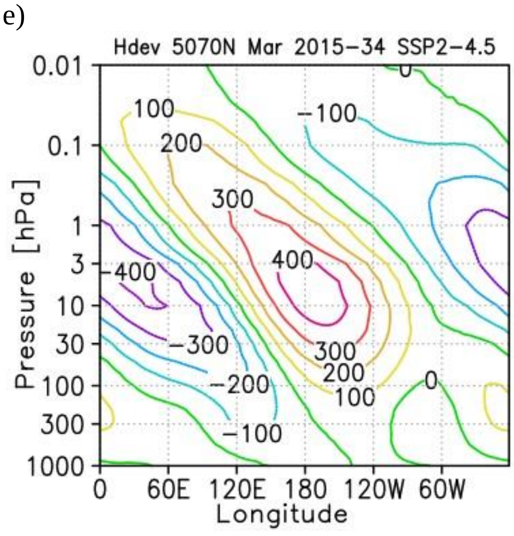
Hdev 5070N Mar 2015−34 SSP2-4.5
Pressure [hPa]
0.01
0.1
1
3
10
30
100
300
1000
Longitude
0
60E
120E
180
120W
60W
100
−100
200
300
400
−400
−300
−200
300
200
100
0
−100

f)

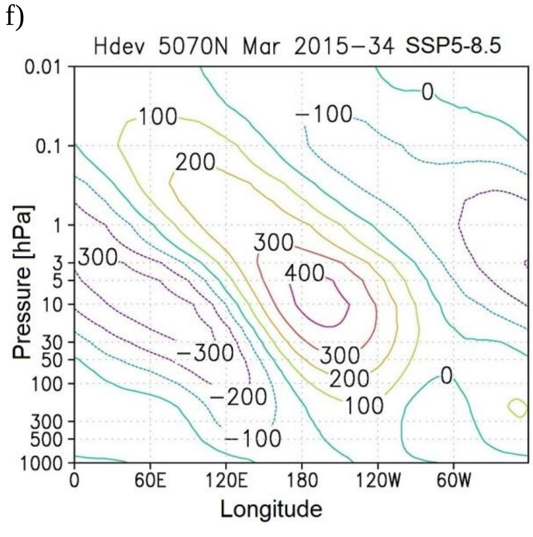
Hdev 5070N Mar 2015−34 SSP5-8.5
Pressure [hPa]
0.01
0.1
1
3
5
10
30
50
100
300
500
1000
Longitude
0
60E
120E
180
120W
60W
100
−100
0
200
300
300
400
−300
300
200
0
−200
100
−100

g) h)

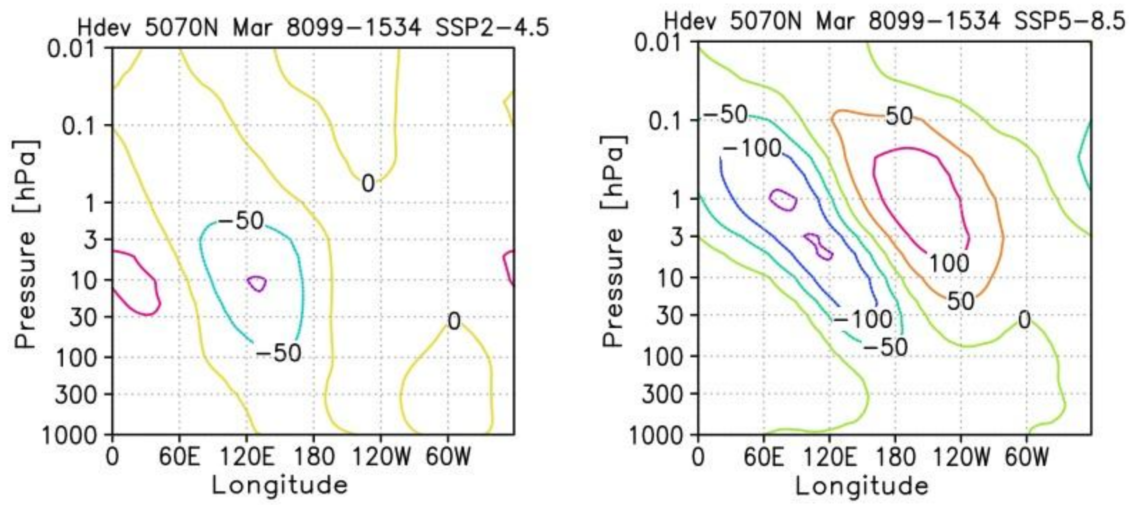

Supplementary Figure S6. Geopotential height January - February mean differences between the same time periods at the pressure levels 10 hPa and 1 hPa under the SSP2-4.5 (a, b) and SSP5-8.5 (c, d). Altitude-longitude cross-section of eddy geopotential height (gpm) averaged across 50°N -70°N latitudes and the time period 2015-2034 March monthly mean under the SSP2-4.5 (e) and SSP5-8.5 (f). Altitude-longitude cross-section of March eddy geopotential height (gpm) averaged across 50°N - 70°N latitudes difference between 2080-2099 and 2015-2034 time periods under the SSP2-4.5 (g) and SSP5-8.5 (h).

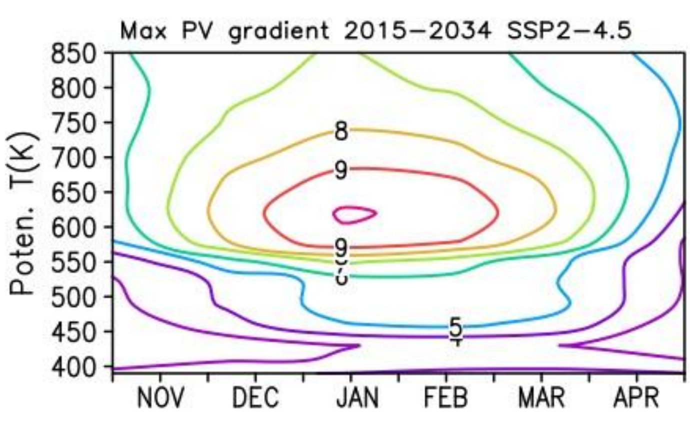

Supplementary Figure S7. Altitude-time diagram (cross-section) of the maximal meridional gradient of potential vorticity ensemble mean (10^{-6} s^{-1} deg^{-1}) in November - April averaged over 2015-2034 in SSP2-4.5 scenario.

a)

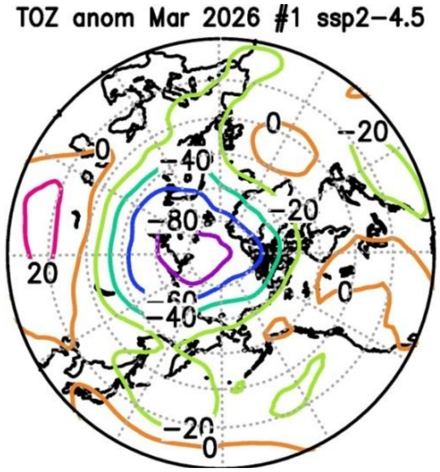
TOZ anom Mar 2026 #1 ssp2-4.5

b)

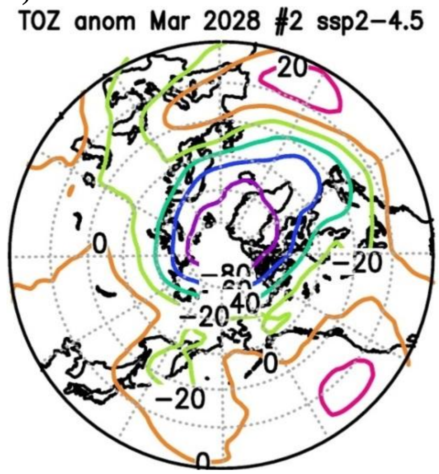
TOZ anom Mar 2028 #2 ssp2-4.5

c)

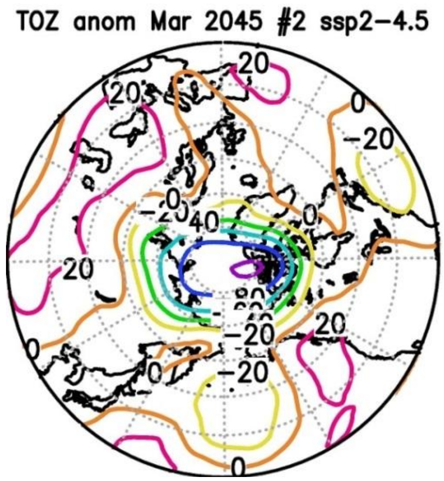
TOZ anom Mar 2045 #2 ssp2-4.5

d)

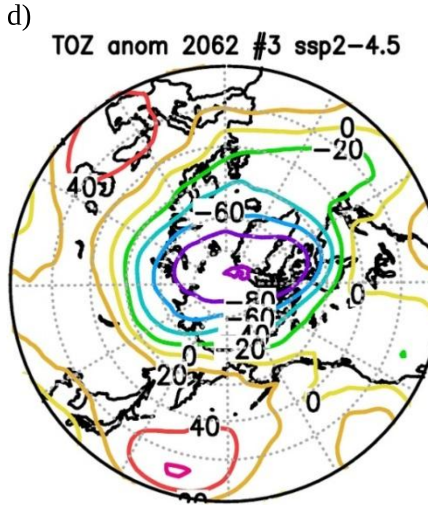
TOZ anom 2062 #3 ssp2-4.5

e)

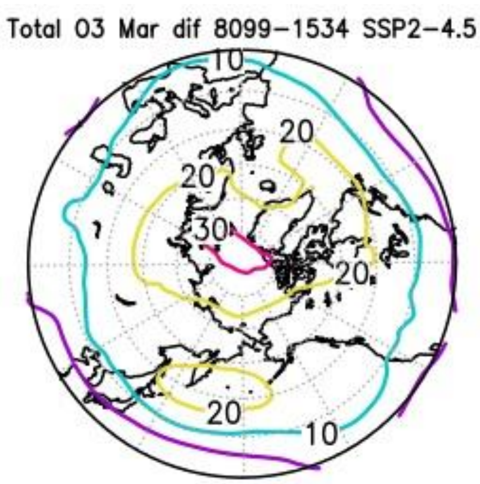
Total O3 Mar dif 8099-1534 SSP2-4.5

f)

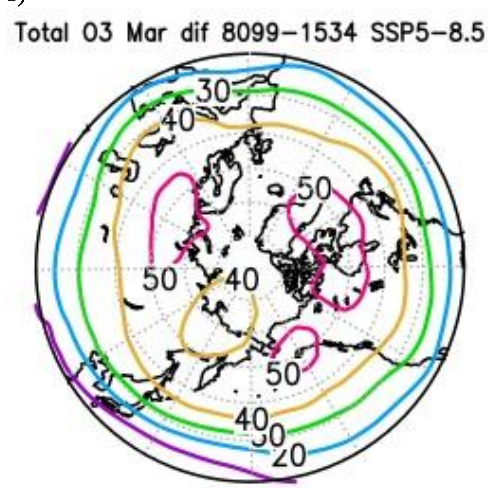
Total O3 Mar dif 8099-1534 SSP5-8.5

g)

h)

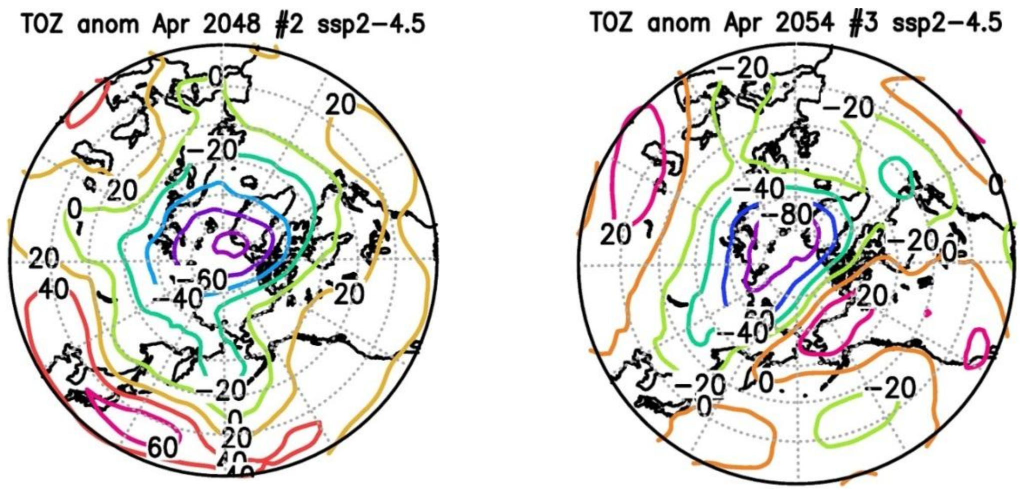

Supplementary Figure S8. The largest negative total column ozone anomalies (DU) in March of 2026 (experiment #1) (a), 2028, 2045 (#2) (b, c), and 2062 (#3) (d) in the SSP2-4.5 scenario**.** Difference in total ozone in March between the time periods 2080-2099 and 2015-2034 for ensemble mean under SSP2-4.5 (e) and SSP5-8.5 scenario (f)**.** The largest negative total column ozone anomalies (DU) in April of 2048 (experiment #2) and April 2054 (#3) in the SSP2-4.5 scenario (g, h)**.**